ANSTO/E683

ANSTO/E683

ansto

APPLICATION OF THE PHOTON-FLUENCE SCALING THEOREM TO ABSORBED DOSE CALORIMETRY FOR BREMSSTRAHLUNG PEAK ENERGY > 1.02 MeV

by

S L SHERLOCK

REPORT E

ISSN 1030-7745
ISBN 0 642 59895 9
August 1989

ISSN 1030-7745
ISBN 0 642 59895 9

The following descriptors have been assigned from the INIS Thesaurus to describe the subject content of this report for information retrieval purposes. For further details please refer to IAEA-INIS-12 (INIS: Manual for Indexing) and IAEA-INIS-13 (INIS: Thesaurus) published in Vienna by the International Atomic Energy Agency.

BREMSSTRAHLUNG; CALORIMETERS; COBALT 60; COMPTON EFFECT; DEPTH DOSE DISTRIBUTIONS; ELECTRON PAIRS; ELECTRON SPECTRA; ENERGY DEPENDENCE; GAMMA DOSIMETRY; GRAPHITE; IONIZATION CHAMBERS; KERMA; PAIR PRODUCTION; PHANTOMS; PHOTONS; RADIATION DOSES; STOPPING POWER; WATER.

EDITORIAL NOTE

The Australian Nuclear Science and Technology Organisation (ANSTO) replaced the Australian Atomic Energy Commission (AAEC) on 27 April 1987. Reports issued after April 1987 have the prefix ANSTO with no change of the symbol (E, M, S or C) or numbering sequence.

AUSTRALIAN NUCLEAR SCIENCE AND TECHNOLOGY ORGANISATION

LUCAS HEIGHTS RESEARCH LABORATORIES

APPLICATION OF THE PHOTON-FLUENCE SCALING THEOREM TO ABSORBED DOSE CALORIMETRY FOR BREMSSTRAHLUNG PEAK ENERGY > 1.02 MeV

by

S L SHERLOCK

ABSTRACT

The determination of absorbed dose in water from a measurement of absorbed dose in graphite is dependent on the use of an ionisation chamber as transfer instrument. Energy dependent response of the transfer instrument leads to errors in the conversion process.

Application of the "photon fluence scaling theorem" allows the ionisation chamber to be placed at points in both media where the photon fluence is the same, hence eliminating problems with energy response.

The theorem is applicable to Compton scattered photons. For photon energies greater than 1.02, pair production alters the photon fluence in such a way as to invalidate the scaling theorem.

In this report the effect of pair production is examined, so that a correction may be applied to the photon fluence scaling theorem. This correction extends application of the theorem for bremsstrahlung spectra up to at least 25 MeV peak energy.

CONTENTS

1. INTRODUCTION

The measurement of absorbed dose for media irradiated by bremsstrahlung with peak energies in the range 1 to 25 MeV has been developed in two quite distinct ways. In the first, absolute determinations have been performed using graphite microcalorimeters, which measure directly in a small absorbing body the temperature rise induced by the absorption of radiation. The second technique measures the ion current induced in a small air cavity, conversion of this quantity to absorbed dose being performed by application of the Bragg-Gray theory. Thus calorimetry determines the absorbed dose in graphite, whilst ionometry determines the absorbed dose in air.

The quantity of practical interest is the absorbed dose in water; water being an acceptable representation of human tissue, e.g. as for treatment of cancer in radiotherapy. In neither calorimetry nor ionometry is the absorbed dose to water measured directly. Consequently, conversion theories are required to obtain absorbed dose in water from absorbed dose in graphite or air.

This report discusses the transfer of absorbed dose from graphite to water. Since the dose conversion method uses an ionisation chamber as transfer instrument, the theory of ionometry must also be considered. This would not be the case if the ionisation chamber energy response was flat over the range of photon energies encountered. However, this is not the case.

In an attempt to bypass the problem of ion chamber energy response, Pruitt and Loevinger [1982] adopted a photon-fluence scaling theorem for Compton-scattered radiation. By means of this theorem, points are established in both media, i.e. graphite and water, where the energy response of the ion chamber is the same. For the purpose of the conversion theory, the energy response of the transfer instrument is then flat.

However, the theory is restricted to Compton absorption processes only. For energies above approximately 200 keV, the Compton photon cross-section depends only on electron density, and is independent of atomic number. However, above 1.02 MeV, the cross-section for pair production increases approximately linearly with photon energy and with the square of the atomic number. At 25 MeV, pair production is a major component of the photon cross-section. Also, above 2.04 MeV, pair production in the field

of the electron (triplet production) commences. These processes modify the bremsstrahlung photon spectra differently in the graphite and water media.

Consequently, the photon fluence congruity established by the Compton scaling theorem is lost. There is then a need to provide either a correction factor to restore the scaling theorem congruence or an alternative to the scaling theorem.

In this report, the effect of pair and triplet production on the photon-fluence scaling theorem is examined. Methods are given for extending the usefulness of the theorem to 25 MeV peak bremsstrahlung spectra.

2. DOSIMETRY THEORY

Subsequent sections of this report apply the dosimetry formalism of Loevinger [1981] to the determination of absorbed dose in water by calorimetry in graphite. Some improvement in clarity of the developed theory may be achieved by using this section to introduce the relevant theory and dosimetric techniques.

2.1 Absorbed Dose Calorimetry

The Urquhart [1978] graphite calorimeter comprises a nested set of ovens enclosing an absorbing element. This element is 20 mm in diameter, contains 1677.7 mg of graphite, density 1.8 $g.cc^{-1}$ and contains a heater winding. The ovens are also graphite, which both ensure constant temperature of the absorber and provide the absorber with a relatively uniform scattering environment. Embedded in the absorber is a thermistor which detects temperature changes.

By comparing the radiation induced heating to that produced by passing a known electrical current through the absorber heater winding, the absorbed dose to graphite may be determined both directly and absolutely. The assumption is made that all the radiation energy absorbed by the detecting element is degraded to heat.

2.2 Ionometry

Ion chambers comprise an air cavity into which is introduced charge collection electrodes. Charges produced in the air cavity are separated by a polarising potential placed across the electrodes, giving rise to an ionisation current. Production of charges arises from the passage of

secondary electrons through the air, the electrons being released from the surrounding medium and wall of the cavity. Photon interactions in the gas are negligible.

Since the process of ionisation of air depends on the energy spectrum of secondary electrons crossing the cavity, ion chambers have an energy dependent response. This property gives rise to the complexities of absorbed dose cavity theory.

By contrast, the calorimeter has a flat energy response.

2.3 Dosimetric Quantities

The interaction of bremsstrahlung beams with matter is complex. Modern theory does not lead to a rigorous determination of absorbed dose. Accordingly, some assumptions must be made which cannot be analytically justified. Despite these difficulties, analysis using the following strategy is productive.

The transfer of energy from photons to the medium takes place in two steps.

- the transfer of photon energy to atomic electrons
- the transfer of energy from the secondary electrons to the medium.

For the first step, define the mass energy absorption coefficient μ_{en}/ρ by

$$\frac{\mu_{en}}{\rho} = \frac{1}{E\rho} \frac{dE_k}{d\ell} (1-g) \qquad (1)$$

where E is the sum of the energy for all photons incident on an element of matter, ρ is the density of the matter, dE_k the sum of the kinetic energies for all the charged particles produced in the layer of thickness $d\ell$, and g is the fraction of dE_k lost from the element as bremsstrahlung.

The second step is the process of energy loss from the secondary electrons to the medium, which is characterised by the mass stopping power S/ρ defined as

$$\frac{S}{\rho} = \frac{1}{\rho} \frac{dE_s}{d\ell} \qquad (2)$$

where dE_s is the average energy lost by a charged particle of specified energy in traversing a path length $d\ell$ in the medium.

Returning to the process of energy transfer from photons to secondary electrons, define 'kerma' K (kinetic energy released per unit mass m)

$$K = \frac{dE_K}{dm} \tag{3}$$

and photon energy fluence ψ by

$$\psi = \frac{dE_F}{da} \tag{4}$$

where dE_F is the sum of photon energies entering area da. Then for mono-energetic photons

$$\frac{K}{\psi} = \frac{dE_K}{dm} \frac{da}{dE_F}$$

$$= \frac{1}{\rho} \frac{1}{dE_F} \frac{dE_K}{d\ell}$$

$$= \frac{1}{E\rho} \frac{dE_K}{d\ell}$$

$$= \frac{\mu_{tr}}{\rho} \tag{5}$$

Here, $\frac{\mu_{tr}}{\rho}$ is the mass energy transfer coefficient. With K^{col} and K^{rad} denoting the collision and radiative components of total kerma K, then

$$K = K^{col} + K^{rad} \tag{6}$$

and $$K^{col} = \psi \frac{\mu_{en}}{\rho} \tag{7}$$

i.e. the mass energy absorption coefficient is the ratio of collison kerma to photon energy fluence.

For a bremsstrahlung spectrum it follows that

$$K^{col} = \int_0^\infty \frac{\mu_{en}}{\rho}(h\nu) \frac{d\psi(h\nu)}{dh\nu} dh\nu \tag{8}$$

$$= \frac{\int_0^\infty \frac{\mu_{en}}{\rho} \frac{d\psi}{dE} dE}{\int_0^\infty \frac{d\psi}{dE} . dE} . \psi(\infty)$$

$$= \frac{\bar{\mu}_{en}}{\rho} \psi(\infty) \tag{9}$$

Consider again the energy transferred to the medium from the secondary electrons, i.e. the absorbed dose. Absorbed dose D is related to the stopping power in the medium, i.e. the absorbed dose at a point dE/dm depends on the flux of secondary electrons through that point. These electrons arise from a volume of matter surrounding the point, and hence depend on the photon fluence throughout that volume.

By contrast, the kerma at a point is uniquely determined by the photon energy fluence at that point. Both kerma and absorbed dose have the units energy per unit mass, i.e. J/kg, special name Gray. Define the quantity β as the quotient of absorbed dose to kerma

$$\beta = \frac{D}{K^{col}} \tag{10}$$

Then

$$D = \beta K^{col}$$

$$= \beta \frac{\bar{\mu}_{en}}{\rho} \psi(\infty) \tag{11}$$

The equations (1) through (11) are fundamental for dosimetry theory and will now be applied in Section 3 of this report.

3. GRAPHITE TO WATER DOSE CONVERSION THEORY

Stated generally, the problem at hand is to determine the absorbed dose in one medium given that the absorbed dose is known in a second medium.

For example, the dose in graphite is known by calorimetry. In the same incident photon field, what then would be the absorbed dose in water? Comparing the two media, the photon energy fluence, mass energy absorption coefficients and mass stopping powers will all vary. In the method of dose conversion to be described here, these factors will all affect the operation of the dose transfer ionisation chamber. Accordingly, the response of the ion chamber in differing media must be understood.

Consider first the energy dependent response of a thick-walled ionisation chamber. From the Bragg-Gray cavity theory, if the chamber was all wall material,

$$\frac{D_{wall}}{D_{gas}} = \left(\frac{\bar{S}}{\rho}\right)^{wall}_{gas} \qquad (12)$$

where D_{wall} is the absorbed dose at the chamber centre, D_{gas} is the absorbed dose to the air in the chamber, at the same point, and $\left(\frac{\bar{S}}{\rho}\right)^{wall}_{gas}$ is is the ratio of mean mass stopping powers, wall to gas. Note that the volume of the chamber is assumed to have negligible effect, i.e. perturbation of the photon and electron fluences is small.

Now D_{gas} is given identically by

$$D_{gas} = J_{gas} \left(\frac{W}{e}\right)_{gas} \qquad (13)$$

where J_{gas} is the charge collected for unit mass of gas in the cavity, and $\left(\frac{W}{e}\right)_{gas}$ is the mean energy expended in the gas per unit charge produced.

Combining equations (12 and (13) yields

$$D_{wall} = J_{gas} \left(\frac{W}{e}\right)_{gas} \left(\frac{\bar{S}}{\rho}\right)^{wall}_{gas} \qquad (14)$$

Now the Bragg-Gray theory which leads to equation (14) applies to an isotropic radiation distribution, e.g. a β source uniformly dispersed in an infinite medium. For a bremsstrahlung beam, the perturbation of the medium by the cavity must be considered. Adopting the Spencer-Attix [1955] scheme equation (14) becomes

$$D_{wall} = J_{gas} \left(\frac{W}{e}\right)_{gas} \left(\frac{\bar{L}}{\rho}\right)^{wall}_{gas} {}_{cav}(\psi)^{wall}_{gas} \qquad (15)$$

where $\left(\frac{\bar{L}}{\rho}\right)^{wall}_{gas}$ is the weighted mean restricted collision mass electron stopping power ratio wall to gas, and ${}_{cav}(\psi)^{wall}_{gas}$ is the ratio of photon fluence at the centre of the cavity when the medium replaces the cavity, to the value when the cavity is filled with gas. Thus ${}_{cav}(\psi)^{wall}_{gas}$ is a a replacement factor; it corrects for the replacement of the wall by the gas in the cavity.

Recall that the chamber is "thick walled". The "thick wall" has linear dimensions greater than the range of any secondary electron generated in the wall material. In this way, only electrons generated in the wall can traverse the cavity and hence contribute to J_{gas}.

If this thick-walled chamber is placed in a medium made from the same material then the absorbed dose to the medium at the chamber centre, D_{med}, is given by

$$D_{med} = J_{gas} \left(\frac{W}{e}\right)_{gas} \left(\frac{\bar{L}}{\rho}\right)^{med}_{gas} {}_{cav}(\psi)^{med}_{gas} \qquad (16)$$

Equation (16) is the basis of the dose transfer experiment, i.e. determining the absorbed dose to water from the absorbed dose in graphite, with a thick-walled chamber as dose transfer instrument.

The steps in the transfer process are:

- determine the dose to graphite D_{graph} using the graphite microcalorimeter

- place a graphite walled ion chamber in a graphite phantom representing the calorimeter
- with the ion chamber centred at the same point as the calorimeter absorber, determine a calibration N_{graph} of the ion chamber response such that

$$N_{graph} = \frac{cal^{D}graph}{cal^{J}gas} \tag{17}$$

- with the graphite "thick-wall" build-up cap in place, determine the chamber response in water, i.e. ${}_{phantom}{}^{J}gas$.

To determine the dose in a solid graphite cap when the cap is in water, i.e. in phantom, first recall from equation (11).

$${}_{phantom}{}^{D}graph = \beta_{graph} \left(\frac{\bar{\mu}_{en}}{\rho}\right)_{graph} {}_{phantom}\psi(\infty) \tag{18}$$

Here ${}_{phantom}\psi(\infty)$ is the photon fluence at the centre of a solid graphite cap placed at the measurement point in water.

Also from equation (11) at the same point as equation (18), but in unperturbed water (i.e. no cavity),

$$D_{water} = \beta_{water} \left(\frac{\bar{\mu}_{en}}{\rho}\right)_{water} {}_{water}\psi(\infty) \tag{19}$$

Taking the ratio of equation (19) to equation (18)

$$D_{water} = {}_{phantom}{}^{D}graph \left(\beta \frac{\bar{\mu}_{en}}{\rho}\right)_{graph}^{water} \psi(\infty)_{phantom}^{water} \tag{20}$$

Equation (20) is particularly useful. D_{water} is the absorbed dose at a point in water, which is the quantity of interest. Also, ${}_{phantom}{}^{D}graph$ can be found from calorimetry, using an ion chamber as transfer instrument from the solid graphite calorimeter to the graphite in the water phantom.

Consider now the effect of using an ion chamber as transfer instrument. Equation (20) can be related to ion chamber response J_{gas} by equation (15), viz:

$$ {}_{\text{phantom}}D_{\text{graph}} = \text{phantom}\left\{ J_{\text{gas}} \left(\frac{W}{e}\right)_{\text{gas}} \left(\frac{\bar{L}}{\rho}\right)^{\text{graph}}_{\text{gas}} \text{cav}(\psi)^{\text{graph}}_{\text{gas}} \right\} \quad (21) $$

Then substituting (21) in (20) yields

$$ D_{\text{water}} = \text{phantom}\left\{ J_{\text{gas}} \left(\frac{W}{e}\right)_{\text{gas}} \left(\frac{\bar{L}}{\rho}\right)^{\text{graph}}_{\text{gas}} \text{cav}(\psi)^{\text{graph}}_{\text{gas}} \right\} \left(\beta \frac{\bar{\mu}_{\text{en}}}{\rho}\right)^{\text{water}}_{\text{graph}} \psi(\infty)^{\text{water}}_{\text{phantom}} \quad (22) $$

Recall that in equation (17), a chamber calibration factor in graphite N_{graph} has been determined by calorimetry applying equation (15) to the graphite-walled ion chamber placed in a graphite phantom.

$$ {}_{\text{graph}}D_{\text{graph}} = \text{graph}\left\{ J_{\text{gas}} \left(\frac{W}{e}\right)_{\text{gas}} \left(\frac{\bar{L}}{\rho}\right)^{\text{graph}}_{\text{gas}} \text{cav}(\psi)^{\text{graph}}_{\text{gas}} \right\} \quad (23) $$

Now heuristically assume that

$$ \text{phantom}\left\{ \left(\frac{W}{e}\right)_{\text{gas}} \left(\frac{\bar{L}}{\rho}\right)^{\text{graph}}_{\text{gas}} \text{cav}(\psi)^{\text{graph}}_{\text{gas}} \right\} = \text{graph}\left\{ \left(\frac{W}{e}\right)_{\text{gas}} \left(\frac{\bar{L}}{\rho}\right)^{\text{graph}}_{\text{gas}} \text{cav}(\psi)^{\text{graph}}_{\text{gas}} \right\} \quad (24) $$

Then from equations (22) and (23)

$$ \frac{D_{\text{water}}}{{}_{\text{phantom}}J_{\text{gas}}} = \frac{{}_{\text{graph}}D_{\text{graph}}}{{}_{\text{graph}}J_{\text{gas}}} \left(\beta \frac{\bar{\mu}_{\text{en}}}{\rho}\right)^{\text{water}}_{\text{graph}} \psi(\infty)^{\text{water}}_{\text{phantom}} \quad (25) $$

Equation (25) is quite general. If the point of reference for the dose in graphite is taken as that determined by the calorimeter, then from equation (17),

$$ \frac{{}_{\text{graph}}D_{\text{graph}}}{{}_{\text{graph}}J_{\text{gas}}} = N_{\text{graph}} \quad (26) $$

Also, define N_{water} by

$$ N_{\text{water}} = \frac{D_{\text{water}}}{{}_{\text{phantom}}J_{\text{gas}}} \quad (27) $$

Then rewriting equation (25) yields

$$N_{water} = N_{graph} \left(\beta \frac{\bar{\mu}_{en}}{\rho}\right)^{water}_{graph} \psi(\infty)^{water}_{phantom} \qquad (28)$$

Equation (28) is identical to that given by Pruitt, Domen and Loevinger [1981] (equation (3)). It is necessary to discuss this latter paper further in order to find a means for using equation (28) in high energy photon beams [$h\nu > 1.02$]. In particular, the authors state:

> "Assume that the chamber has been calibrated in a Cobalt-60 gamma-ray beam in graphite, and is used in water at a point where the photon spectral energy fluence is the same as in graphite".

The conditions required here are obtained by an application of the Compton photon-fluence scaling theorem. This theorem may not hold for high energy bremsstrahlung from linear accelerators.

In this present work, the assumption referred to by Pruitt et al [1981] is given explicit expression in equation (24). The quantities $(\frac{W}{e})_{gas}$ and $cav(\psi)^{graph}_{gas}$ are independent of the medium surrounding the thick-walled graphite chamber. However, $(\frac{\bar{L}}{\rho})^{graph}_{gas}$ is a slowly varying function of the electron energy spectrum in the gas. The electron spectrum in turn is dependent on the photon energy fluence in the volume of the graphite cap. Accordingly, the equality given in equation (24) holds identically if the photon energy fluence at the point of measurement in the water phantom is the same as that in the graphite phantom in which N_{graph} was determined.

The conditions required for equation (24) to hold for high energies is considered in section 5.

4. PHOTON FLUENCE SCALING THEOREM $h\nu < 1.02$

A statement of the photon-fluence scaling theorem for Compton-scattered radiation is given by Pruitt and Loevinger [1982]. The theorem is briefly restated in this section, with specific reference to the ANSTO ^{60}Co absorbed dose measurements.

The use of an ionisation chamber as dose transfer instrument has many advantages, including stability and small detector size. However, its energy dependent response implies that absorbed dose is not proportional to ion current (equation 15).

Thus, if the ion chamber, complete with graphite build-up cap, is to be used for comparing doses in graphite phantom with doses in water phantom, then the photon energy spectrum is required to be the same at the point of measurement in each medium. The scaling theorem provides a relationship between photon fluences in two media irradiated by the same source, provided the radiation interacts with the media by Compton scatter only.

The rule is: all distances and dimensions are to be scaled using:

$$x' = \frac{\epsilon}{\epsilon'} x \tag{29}$$

where x is a length, and ϵ is the electron density and $'$ indicates the second medium. Then for every point P in volume V, there is a corresponding point P′ in volume V′ such that the photon spectral distributions are the same in energy and direction, and the photon fluences are related by

$$\psi_{P'} = (\frac{\epsilon'}{\epsilon})^2 \psi_P \tag{30}$$

Combining equations (29) and (30) yields

$$\psi_{P'} = (\frac{x}{x'})^2 \psi_P \tag{31}$$

and $$\psi_{P'} = (\frac{R}{R'})^2 \psi_P \qquad \text{since } \frac{x'}{R'} = \frac{x}{R} \tag{32}$$

where R, R′, x and x′ are illustrated in Figure 1.

The quantity R is the distance from the source, here considered a point source, to the point P.

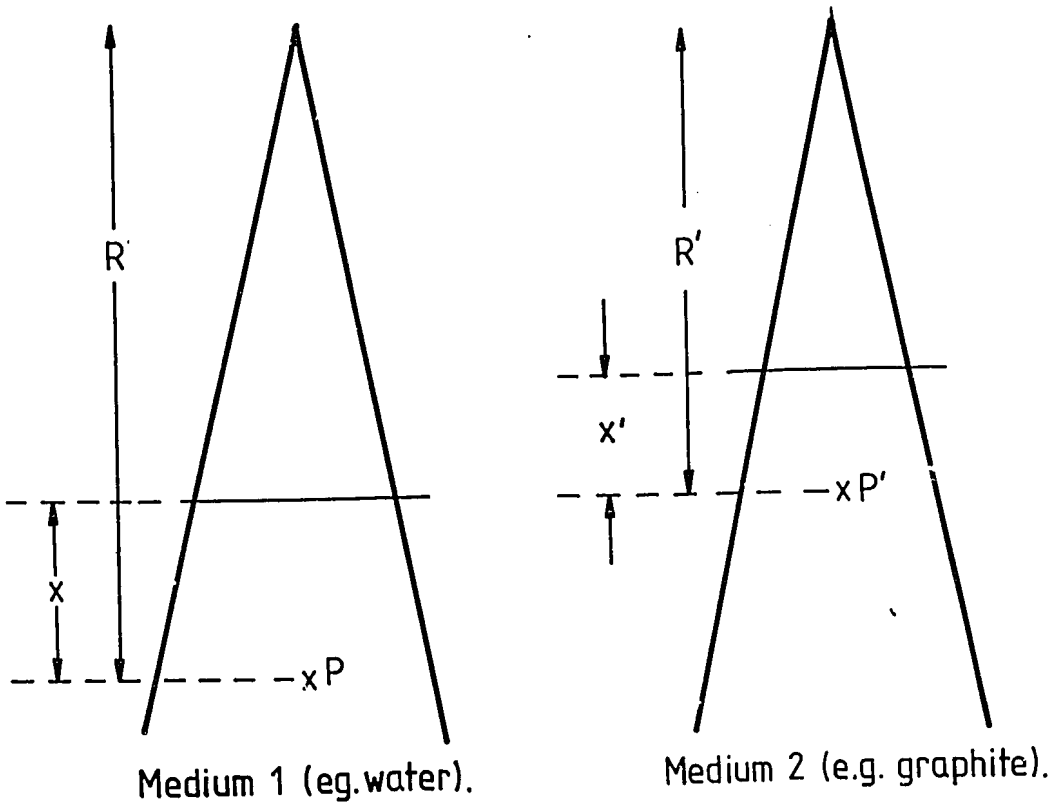

Figure 1. Photon fluence scaling of length.

Consider the dose transfer experiment, graphite to water. Taking the mass densities of water and graphite as 1.0 $g.cm^{-3}$ and 1.7 $g.cm^{-3}$, the number of electrons per unit volume are $.555N_A$ and $.849N_A$ respectively, N_A being Avogadros' number. The scaling factor is then 1.530.

With R' = 100 cm for the graphite calorimeter, then for the water phantom R = 153 cm. The field width scales in the same manner, hence there is no need to change the collimator setting.

The depth of the absorber in the ANSTO graphite calorimeter is 5 $g.cm^{-2}$, or with ρ_{graph} = 1.7 $g.cm^{-3}$, 2.94 cm. The scaled depth in water is then 2.94 x 1.53 = 4.5 cm. In Urquharts report [1978], the ion chamber is placed at a depth of 5.0 cm in water. Thus the scaled depth and the depth expressed in $g.cm^{-2}$ are not equivalent.

5. PHOTON FLUENCE SCALING THEOREM $h\nu > 1.02$

For photon energies greater than 1.02 MeV, the effect of pair production on the scaling theorem must be considered. Pair production is responsible for a large fraction of the absorption process at higher energies (Table 1).

Table 1: Relative Importance of Pair Production at 20 MeV (NBS-29) [1969]

Cross Section at 20 MeV (b/atom)			
Element	Pair	Total	Fraction
H	.0033	.0036	.92
C	.117	.314	.37
O	.208	.469	.45

The energy balance equation for pair production is:

$$h\nu - 2m_o c^2 = T_+ + T_-$$

where T_+ is the kinetic energy of the positron and T_- the kinetic energy of the electron. At annihilation of the positron, two 0.511 MeV photons are produced.

Since the incident photon ($h\nu$) disappears, the requirement for scaling the field width does not apply. However, the depth scaling is upset. The photon fluence is modified by the pair attenuation coefficient, which also depends on atomic number. Since the elements involved are H, C and O, and pair production varies with $Z^2\ h\nu$, it is difficult to see how identical photon fluences could be found in graphite and water at any point.

Recall for a moment the dose transfer experiment for a thick walled chamber. The requirement for identical photon spectra in graphite and water arose from the requirement (equation 24) that

$$\left[\left(\frac{\bar{L}}{\rho}\right)_{\text{gas}}^{\text{graph}} \right]_{\text{phantom}}^{\text{graph}} = 1 \qquad (33)$$

The condition that the photon spectra be identical for equation (33) is in fact too restrictive. With $\phi(E)\ dE$ the number of secondary electrons with energies in the range E to E +dE and E_o the peak electron energy generated by the bremsstrahlung spectrum,

$$\frac{\bar{L}}{\rho} = \frac{\int_{\Delta}^{E_o} \phi(E)\ (\frac{L(E)}{\rho})\ dE}{\int_{\Delta}^{E_o} \phi(E)\ dE} \tag{34}$$

Thus equation (33) is met if

$$\left[\left\{ \frac{\int_{\Delta}^{E_o} \phi(\frac{L}{\rho})\ dE}{\int_{\Delta}^{E_o} \phi\ dE} \right\}_{gas}^{graph} \right]_{phantom}^{graph} = 1 \tag{35}$$

The condition represented by equation (35) is actually somewhat relaxed, as the photon spectra do not have to be identical to obtain this result. Although the pair production in the two media virtually guarantees the photon spectra will be different, there may yet exist a point in each medium where equation (35) holds. Certainly, the immediate problem is to study the effect of pair production on the photon spectrum.

An alternative approach is to determine a correction factor which allows for the differing energy response of the ion chamber in phantom and graphite. Considering equation (24), define η such that

$$\eta = \left\{ (\frac{W}{e})_{gas}\ (\frac{\bar{L}}{\rho})_{gas}^{graph}\ {}_{cav}(\psi)_{gas}^{graph} \right\}_{phantom}^{graph} \tag{36}$$

Then equation (28) becomes

$$N_{water} = N_{graph}\ \eta\ (\beta \frac{\bar{\mu}_{en}}{\rho})_{graph}^{water}\ \psi(\infty)_{phantom}^{water} \tag{37}$$

Again, taking $(\frac{W}{e})_{gas}$ and ${}_{cav}(\psi)_{gas}^{graph}$ to be independent of photon spectrum, equation (36) reduces to

$$\eta = \left[(\frac{\bar{L}}{\rho})_{gas}^{graph} \right]_{phantom}^{graph} \tag{38}$$

The quantity η is amenable to calculation, either by analytical or Monte Carlo methods.

Having established the nature of the problem in photon fluence scaling with pair production, it remains to analyse the various approaches in the following sections.

6. PHOTON SPECTRUM MODIFICATION BY PAIR PRODUCTION

In this section, the photon spectrum for $E_o > 1.02$ MeV is examined in an attempt to find homologous points in graphite and water such that η (equation (36)) is unity.

Consider an incident bremsstrahlung spectrum $d\psi_o/dh\nu$. Then at a depth d in a given medium, the photon spectrum $d\psi/dh\nu$ is given by

$$\left.\frac{d\psi}{dh\nu}\right|_{medium} = e^{-\mu_k d} e^{-\mu_c d} \frac{d\psi_o}{dh\nu} + S_c + S_k \qquad (39)$$

where $e^{-\mu_k d}$ and $e^{-\mu_c d}$ give the loss of photons from the incident beam due to pair production and Compton scatter respectively; and S_c and S_k are the Compton scattered and annihilation photons reaching the point of interest.

Subsequent to their production, the absorbed dose due to the annihilation quanta is again independent of atomic number. The absorption process then depends on the electron density; it is therefore reasonable to assume that the quanta given by S_k obey the photon fluence scaling theorem.

Applying equation (39) to spectra in graphite and water phantoms yields

$$\left[\frac{d\psi}{dh\nu}\right]_{phantom}^{graph} = \left[e^{-\mu_k d} e^{-\mu_c d} \frac{d\psi_o}{dh\nu} + S_c + S_k\right]_{phantom}^{graph} \qquad (40)$$

The term $S_c + S_k$ is typically an order of magnitude less than $e^{-\mu_k d} e^{-\mu_c d} \frac{d\psi_o}{dh\nu}$.

Therefore, on expanding equation (40) in series form, dropping higher order terms and recognising that second order terms cancel out yields.

$$\left[\frac{d\psi(h\nu)}{dh\nu} \right]_{phantom}^{graph} = \frac{e^{-\mu_k(h\nu)_{graph}\, d_{graph}}}{e^{-\mu_k(h\nu)_{phantom}\, d_{phantom}}} \tag{41}$$

Since the number of charged particles depends on the loss of photons, then define cross-section $d\sigma(h\nu)/dE$ as the probability that a photon in the energy range $h\nu$ to $h\nu + dh\nu$ produces an electron (or positron) of energy in the range E to E + dE. Then the electron spectrum is just

$$\phi(E) = \int \frac{d\psi(h\nu,d)}{dh\nu} \frac{d\sigma(h\nu)}{dE}\, dh\nu \tag{42}$$

Then from equation (34)

$$\frac{L}{\rho} = \frac{\int_E \frac{L(E)}{\rho} \int_{h\nu} \frac{d\psi}{dh\nu}(h\nu,d) \frac{d\sigma(h\nu)}{dE}\, dh\nu\, dE}{\int_E dE \int_{h\nu} \frac{d\psi(h\nu,d)}{dh\nu} \frac{d\sigma(h\nu)}{dE}\, dh\nu} \tag{43}$$

Combining equations (41) and (43), then substituting in equation (38) yields

$$\eta = \frac{\int_E \frac{L_{graph}}{\rho} \int_{h\nu} \left[\frac{d\psi}{dh\nu} \right]_{phantom}^{graph} \frac{d\psi_{phantom}}{dh\nu} \frac{d\sigma_{graph}}{dE}\, dh\nu\, dE}{\int_E \frac{L_{gas}}{\rho} \int_{h\nu} \left[\frac{d\psi}{dh\nu} \right]_{phantom}^{graph} \frac{d\psi_{phantom}}{dh\nu} \frac{d\sigma_{graph}}{dE}\, dh\nu\, dE} \Bigg/ \frac{\int_E \frac{L_{graph}}{\rho} \int_{h\nu} \frac{d\psi_{phantom}}{dh\nu} \frac{d\sigma_{graph}}{dE}\, dh\nu\, dE}{\int_E \frac{L_{gas}}{\rho} \int_{h\nu} \frac{d\psi_{phantom}}{dh\nu} \frac{d\sigma_{graph}}{dE}\, dh\nu\, dE} \tag{44}$$

Note that the restriction placed on equation (44) by the application of equation (41) is that, for a water phantom,

$$d_{phantom} = 1.530\, d_{graph} \tag{45}$$

Recall that the purpose of this exercise is to determine the deviation of η from unity, or, preferably to make η equal to unity. Inspection of equation (44) shows that η is unity when $\left(\frac{d\psi}{dh\nu}\right)^{graph}_{phantom}$ is constant, i.e. does not vary with $h\nu$.

Values of $\left(\frac{d\psi}{dh\nu}\right)^{graph}_{phantom}$ were computed using monochromatic photon data from NBS 29 [1969]. The depth in graphite used was 2.94 cm, corresponding to the ANSTO calorimeter measuring point. Table 2 gives the results for graphite bulk density of 1.7 $g.cc^{-3}$, and Table 3 gives the results for grain density 2.25 $g.cm^{-3}$.

Table 2: Values of $\left(\frac{d\psi}{dh\nu}\right)^{graph}_{phantom}$ at various depths in water phantom, graphite bulk density 1.7 $g.cm^{-3}$. Depth in graphite 2.94 cm.

$\left(\frac{d\psi}{dh\nu}\right)^{graph}_{phantom}$	ρ_{graph} : 1.7 $g.cm^{-3}$			
	Depth in Water (cm)			
$h\nu$ (MeV)	3	4.15	4.5	6.0
5	.9972	1.0001	1.0010	1.0048
10	.9943	1.0001	1.0019	1.0096
15	.9924	1.0001	1.0024	1.0126
20	.9910	1.0001	1.0029	1.0150
30	.9891	1.0001	1.0035	1.0181

Table 3: Values of $\left(\frac{d\psi}{dh\nu}\right)^{graph}_{phantom}$ at various depths in water phantom, graphite grain density 1.7 $g.cm^{-3}$. Depth in graphite 2.94 cm.

$\left(\frac{d\psi}{dh\nu}\right)^{graph}_{phantom}$	ρ_{graph} : 2.25 $g.cm^{-3}$			
	Depth in Water (cm)			
$h\nu$ (MeV)	3	4.5	5.5	6.0
5	.9938	.9976	1.0002	1.0014
10	.9876	.9951	1.0002	1.0027
15	.9835	.9935	1.0002	1.0035
20	.9806	.9923	1.0002	1.0042
30	.9763	.9906	1.0002	1.0051

Inspection of Tables 2 and 3 show that there are indeed values of $d_{phantom}$ for which $\left(\frac{d\psi}{dh\nu}\right)_{phantom}^{graph}$ is constant, with the corollary that η equals unity.

In the case of graphite density 1.70 cm^{-3}, η is unity at 4.15 cm depth. In section 4, it was shown that the photon fluence scaling theorem required a depth of 4.5 cm in the phantom. At this latter depth, $\left(\frac{d\psi}{dh\nu}\right)_{phantom}^{graph}$ does vary slowly.

However, it should be noted that bremsstrahlung spectra have a mean photon energy of approximately 0.4 E_o, so that they are weighted toward lower energies. The effect of this is to make the integrals in equation (43) vary even more slowly.

The conclusion may be drawn that the effect of pair production on the photon fluence scaling theorem is negligible.

7. DIRECT COMPUTATION OF η

Application of the photon-fluence scaling theorem for $h\nu > 1.02$ requires consideration of the effect of pair production on the quantity η (equation 38).

In section 6, it was shown that homologous points could be found in graphite and water phantoms such that η was unity. That such points exist is purely fortuitous.

A more rigorous approach, applicable to arbitrary depths both in graphite and water phantoms, is to compute η from known physical data. This calculation can be performed either analytically or by Monte Carlo techniques.

Cunningham and Schulz [1984] have given an analytical method for the calculation of mean stopping powers. Their procedure was followed, using the bremsstrahlung spectrum from a Sagittaire 25 MV linear accelerator (Levy, et alia, 1974).

The Sagittaire spectrum was first filtered through a 4 cm aluminium beam flattener, then two primary spectra generated. One at a depth of 8 cm in graphite, the second at the scaled depth of 12.2 cm in water. No attempt was made to add the scatter back into these primary beams. In retrospect,

it was an error to filter this beam through the aluminium beam flattener, as filtration had already been included in this spectrum. However, the purpose of this exercise is to determine the effect of spectral differences in the two media, so the interpretation of the results remains unambiguous.

The depth of 8 cm in graphite was chosen to ensure that full transient electronic equilibrium was established. This step minimises errors resulting from not considering electron transport in the Cunningham and Schulz [1984] approximation. Also, the corresponding depth of 12.2 cm in water approximates the treatment depth appropriate to this energy in cancer therapy. (Also, it is the depth obtained from the photon fluence scaling theorem).

The calculation of equation (43) took into account photoelectric absorption (negligible), Compton absorption and pair and triplet production. The electron spectrum was aged using the CSDA approximation, and the Spencer-Attix [1955] correction for delta-rays applied.

However, the electron spectrum generated by absorption of annihilation quanta was not included in this calculation. As a result of this and the somewhat hardened photon spectrum, the mean of the aged electron spectrum was somewhat higher than expected for a 25 MeV bremsstrahlung photon beam.

The result obtained here for $\frac{\bar{L}}{\rho}_{graph}$ was .931, while a value of .968 has been given in the AAPM protocol [1983]. It should be noted that the latter value was computed for primary photons only, i.e. no photon spectrum modification with depth. In this report, the modification of the photon spectrum by filtration through the medium is the whole point of the analysis. To the extent that the Compton scatter and annihilation photons have been neglected, this analysis is compromised.

However, since the photon fluence scaling theorem was applied, this compromise should be of no significance.

For calculations of η for arbitrary depths, the Compton scatter and annihilation photons should be included. Best procedure for this would be to apply a recognised Monte Carlo code, such as EGS4 [1984].

Results of the present calculation are given below.

25 MV Bremsstrahlung Beam				
d_{graph} (cm)	$d_{phantom}$ (cm)	$\frac{\bar{L}}{\rho}_{graph}$	$\frac{\bar{L}}{\rho}_{phantom}$	η
8	12.2	.93098	.93137	.9996

The correction factor η is very close to unity. Since pair production is highest for this energy, it may be concluded that for all energies between 1.02 and 25 MeV the photon-fluence scaling theorem is valid. This result supports the observations made in section 6.

8. REFERENCES

Fruitt, J.S. and Loevinger, R. [1982] - The photon-fluence scaling theorem for Compton-scattered radiation. Med. Phys. 9(2), March/April, 176-179, 1982.

Loevinger, R. [1981] - A formalism for calculation of absorbed dose to a medium from photon and electron beams. Med. Phys. 8(1), January/February, 1-12, 1981.

Urquhart, D.F. [1978] - The Australian Commonwealth standard of measurement for absorbed radiation dose. AAEC/E455.

Spencer, L.V. and Attix, F.H. [1955] - A theory of cavity ionisation. Radiat. Res. 3, 239 [1955].

Pruitt, J.S., Domen, S.R. and Loevinger, R. [1981] - The graphite calorimeter as a standard of absorbed dose for Cobalt-60 gamma radiation. Journal of Research of the National Bureau of Standards, Vol.86, No.5, September/October, 495-502, 1981.

Cunningham, J.R. and Schulz, R.J. [1984] - On the selection of stopping-power and mass energy-absorption coefficient ratios for high-energy x-ray dosimetry. Med. Phys. 11(5), September/October, 618-623, 1981.

Task Group 21, Radiation Therapy Committee, American Association of Physicists in Medicine [1983] - A protocol for the determination of absorbed dose from high-energy photon and electron beams. Med. Phys. 10(6), November/December, 741-771, 1983.

Levy, L.B, Waggener, R.G., McDavid, W.D. & Payne, W.H. [1974] - Experimental and calculated bremsstrahlung spectra from a 25-MeV linear accelerator and a 19-MeV betratron. Medical Physics, Vol.1, No.2, 62-67, 1974.

EGS4 [1985] Nelson, W.R., Hirayama, H. and Rogers, W.O. - The EGS4 code system. SLAC-Report-265, December 1985. National Technical Information Service, U.S. Department of Commerce, 5285 Port Royal Road, Springfield, Virginia 22161.

NBS 29 [1969] Photon cross-sections, attenuation coefficients, and energy absorption coefficients from 10 keV to 100 GeV. U.S Department of Commerce National Bureau of Standards.